Pure Appl. Geophys. 177 (2020), 5833–5844

https://doi.org/10.1007/s00024-020-02601-1

Pure and Applied Geophysics

Longitudinal Variation of the Ionospheric Response to the 26 August 2018 Geomagnetic Storm at Equatorial/Low Latitudes

Gustavo A. Mansilla[1,2] and Marta M. Zossi[1,2]

Abstract—We have studied the ionospheric response at near-equator latitudes during the geomagnetic storm of 26 August 2018, which was the strongest geomagnetic disturbance that year (minimum Dst value: −174 nT). For the analysis, we considered the F2-layer critical frequency (foF2) and peak height (hmF2), as well as total electron content (TEC) data for Jicamarca (geographic coordinates: 12° S, 283.2° E; geomagnetic coordinates: 2.26° S, 4.09° W), Saoluis (geographic coordinates: 2.6° S, 315.8° E; geomagnetic coordinates: 5.94° N, 28.5° E), Guam (geographic coordinates: 13.4° N, 144.8° E; geomagnetic coordinates: 5.73° N, 143.2° W) and Libreville (geographic coordinates: 0.39° N, 9.45° E; geomagnetic coordinates: 1.64° N, 82.6° W). First, we observed pre-storm improvements, which could be due to previous moderate geomagnetic activity. Second, only one station (Jicamarca) clearly revealed a prompt penetration electric field (PPEF) effect when Bz turned strongly negative during the initial phase of the storm. Over the stations Saoluis and Guam, a PPEF effect was not evident. These stations presented pre-storm enhancements in foF2. In this case study, disturbed dynamo electric fields appear not to have played a crucial role in increasing electron density near equatorial regions during the recovery phase because the observed disturbances did not correspond with those produced by these electric fields, that is, negative (positive) storm effects on the dayside (night). Third, the increases in electron density observed during recovery are most likely caused by neutral composition changes.

Keywords: Geomagnetic storm, ionospheric parameters, physical mechanisms.

1. Introduction

During geomagnetic storms, there is a magnetospheric energy input into the polar upper atmosphere, which significantly modifies the chemical and dynamics/electrodynamics processes of the ionosphere-thermosphere system. In particular, the equatorial and low-latitude ionosphere exhibits remarkable variations during these events. Significant changes of the F2-layer critical frequency (foF2) from normal values during geomagnetic storms are called ionospheric storms (Buonsanto 1999). Basically, foF2 (proportional to the peak electron density of the F region), can either increase or decrease from its quiet time value during disturbed conditions (the so-called positive or negative ionospheric storms; e.g., Prölss 1995, p. 200).

The ionosphere presents complex disturbance characteristics driven by different interacting physical processes. Prompt penetration electric fields and disturbance dynamo electric fields, neutral winds and subsequent compositional changes, among others, have been reported as physical mechanisms to explain the features of the ionospheric behavior during the different stages of the geomagnetic storms (e.g., Mayr and Volland 1972; Prölss 1987, 1995, 1997; Blanc and Richmond 1980; Fuller-Rowell et al. 1994; Tsurutani et al. 2008; Richmond and Lu 2000; Huang 2013).

In the equatorial region and low latitudes, the storm-time ionospheric disturbed electric fields play an important role in creating the initial ionospheric storm effects. With the starting of the storm's main phase, the interplanetary electric field (IEF) penetrates instantaneously as a prompt penetration electric field (PPEF) from the high latitude to low and equatorial latitudes, which causes a rapid and transient ionospheric disturbance on time scales of 1–2 h. The electric field perturbations associated with the PPEF are mainly directed eastward (westward)

[1] Departamento de Física, Facultad de Ciencias Exactas y Tecnología, Universidad Nacional de Tucumán, Av. Independencia 1800, 4000 San Miguel de Tucumán, Argentina. E-mail: gmansilla@herrera.unt.edu.ar

[2] Consejo Nacional de Investigaciones Científicas y Técnicas, 2290 Godoy Cruz, CABA, Argentina.

during day (night) (e.g., Nishida 1968; Sastri et al. 1997; Fejer et al. 1983, 2008; Abdu et al. 2003; Huang et al. 2007).

The storm-induced disturbance winds further generate a disturbance dynamo electric field (DDEF) at middle and equatorial latitudes, which perturbs the low-latitude and equatorial ionosphere during and up to about a day or two after the onset of a geomagnetic storm (e.g., Blanc and Richmond 1980; Huang et al. 2005a; Zhou et al. 2016).

A majority of studies on the latitudinal or longitudinal dependencies of ionospheric responses are limited to a particular latitude–longitude region, although there are studies on global density distributions. For example, Sahai et al. (2005) studied equatorial and low-latitude F regions in two longitudinal sectors separated by about 12 h in local time (LT) during an intense geomagnetic storm and observed that the two longitudinal sectors considered clearly showed the global nature of the storm-time effects. However, Pedatella et al. (2008) examined the evolution of the longitude structure of the low-latitude ionosphere during different phases of geomagnetic storms and observed electron densities at 12 LT does not indicate significant longitudinal structure of the low-latitude ionosphere during the initial-main phases of the storms. Klimenko et al. (2011) performed a study of the middle- and low-latitude ionospheric effects of geomagnetic storms of 9–14 September 2005 with the Global Self-Consistent Model of the Thermosphere, Ionosphere and Protonosphere. Longitudinal variations between Fortaleza, Brazil (geogr. 3.9° S, 38.45° W; dip angle: −11.7°) and Jicamarca, Peru (geogr. 12.0° S, 76.8° W; dip angle: 0.64°) were addressed by Santos et al. (2012).

Despite ionospheric effects of geomagnetic storms having been extensively studied for decades, a complete understanding is still lacking and remains one of the priorities in near-Earth space physics (e.g., Astafyeva et al. 2015; Zolotukhina et al. 2017 and references therein).

As mentioned by Kuai et al. (2017), "the regional differences of the ionospheric storms have been a research hot spot in these years. American Geophysical Union International Chapman conference discussed the topic of 'longitude and hemispheric dependence of space weather' in November 2012."

For this reason, it is important to continue the study of the effects of geomagnetic storms on the ionosphere, in order to have a full understanding of the physical mechanisms involved during these events.

The principal motivation behind this research is to report the variations of the ionospheric parameters critical frequency of the F2 layer (foF2), their peak height (hmF2) and total electron content (TEC) at near-equator latitudes during the geomagnetic storm that occurred on 26 August 2018, and to investigate the responsible physical mechanisms, i.e., how the disturbed electric fields and global thermospheric neutral compositions contribute to the ionospheric responses. We considered four stations: Jicamarca (geographic coordinates: 12° S, 283.2° E; geomagnetic coordinates: 2.26° S, 4.09° W), Saoluis (geographic coordinates: 2.6° S, 315.8° E; geomagnetic coordinates: 5.94° N, 28.5° E), Guam (geographic coordinates: 13.4° N, 144.8° E; geomagnetic coordinates: 5.73° N, 143.2° W) and Libreville (geographic coordinates: 0.39° N, 9.45° E; geomagnetic coordinates: 1.64° N, 82.6° W). Unfortunately, no data from other stations at equatorial/low latitudes were found in order to perform a more complete study.

2. *Data Sets*

In this paper, we present ionospheric sounding data of the F2-layer critical frequency (foF2) and their peak height (hmF2) at the stations Jicamarca, Saoluis and Guam, and the total electron content (TEC) values at Jicamarca, Saoluis, Guam and Libreville for the storm period 25–27 August 2018, which were obtained from the Digital Ionogram Database (DIDBase; https://giro.uml.edu/didbase/scaled.php). These data are processed by the Digisonde Global Ionosphere Radio Observatory (GIRO), which provides all observable parameters of the ionospheric echoes of more than 60 ionosondes located around the world. All digisonde data are ingested in the Lowell GIRO Data Center (LGDC). TEC values for Libreville station were obtained every

2.5 min from the IONOLAB website (https://www.ionolab.org), which provides the online computation of TEC through the Reg-Est algorithm (see Sezen et al. 2013).

The geographic and geomagnetic coordinates of the stations used are listed in Table 1 (geographic coordinates were converted to geomagnetic coordinates using the International Geomagnetic Reference Field [IGRF] model). Figure 1 shows a map with the geographical locations of the stations used in the study. The component of the interplanetary magnetic field Bz (IMF-Bz), the solar wind speed and the proton density were obtained from the OMNI database (https://omniweb.gsfc.nasa.gov). Hourly values of the Dst index were taken from the World Data Center (WDC) Kyoto, Japan, website (https://wdc.kugi.kyoto-u.ac.jp/dstae/index.html). To study the atmospheric neutral compositional changes, the global [O/N2] maps were used, which provide the global thermospheric neutral composition variations obtained from Global Ultraviolet Imager (GUVI) instrument on board TIMED (Thermosphere, Ionosphere, Mesosphere Energetics and Dynamics) spacecraft. The vertical plasma drifts between 150 and 155 km of the Jicamarca Unattended Long-term Investigations of the Ionosphere (JULIA) radar (https://jro.igp.gob.pe/madrigal/) to analyze prompt penetration electric field effects were considered. We also used the eastward prompt penetration electric field model of the Cooperative Institute for Research in Environmental Sciences (CIRES), based on data from the Advanced Composition Explorer (ACE) satellite, the JULIA radar and the magnetometer from the CHAMP satellite (https://geomag.org/models/PPEFM/RealtimeEF.html), to investigate the PPEF effect in the ionospheric disturbances. This model was run along the longitudinal sector of two representative stations.

Table 1

Geographic and geomagnetic coordinates of the stations used in the analysis

	Geog. lat.	Geog. long.	Geomag. lat.	Geomag. long.	LT
Jicamarca (JI)	−12.0	283.2 E	−2.26	4.09 W	UT −5 h
Sao Luis (SL)	−2.6	315.8 E	5.79	28.58 E	UT −3 h
Guam (GU)	13.4	144.8 E	5.70	143.5 W	UT +10 h
Libreville (LI)	0.39	9.45 E	1.68	82.6 E	UT +1 h

3. Solar Wind and Geomagnetic Condition During 25–27 August 2018

Figure 2 shows the variations of the solar wind parameters Bz IMF component, speed and proton density, and the Dst index for the 25–27 August 2018 storm period. As can be seen, and based on the values of the Dst index, the main phase of the geomagnetic storm started at about 19 UT on 25 August and ended at about 07 UT on 26 August, when Dst reached a minimum value of −174 nT. This storm was followed by a slow recovery. Bz turned strongly negative at about 16 UT on 25 August, and it remained in the range of −17 to −10 nT throughout most of 26 August. This allowed the magnetic reconnection with the Earth's magnetic field, which released large amounts of magnetic energy and strongly disturbed the Earth's magnetosphere. On 27 August, an oscillatory behavior with Bz values between +5 and −5 nT stayed throughout the day. The speed was about 400 km/s on 25 August till 12 UT on 26 August when it started a gradual increase, reaching about 550 km/s around midnight 26/27 August. On 27 August, the speed remained between 550 km/s and 620 km/s. The proton density was increased on 25 August, from about 08 to 13 UT with values in the range 15–24 cm^{-3}. At about 22 UT, it started to increase again, reaching a peak of 32 cm^{-3} at 08 UT on the following day after which it decreased to 5 cm^{-3} at 11 UT. Afterwards, there was a secondary enhancement to about 22 cm^{-3} at around 13 UT. On 27 August, values close to 3 cm^{-3} were observed the whole day.

4. Storm-Time Ionospheric Response at Near-Equator Latitudes

In order to analyze the influence of the storm that occurred on 26 August 2018 on the near-equatorial

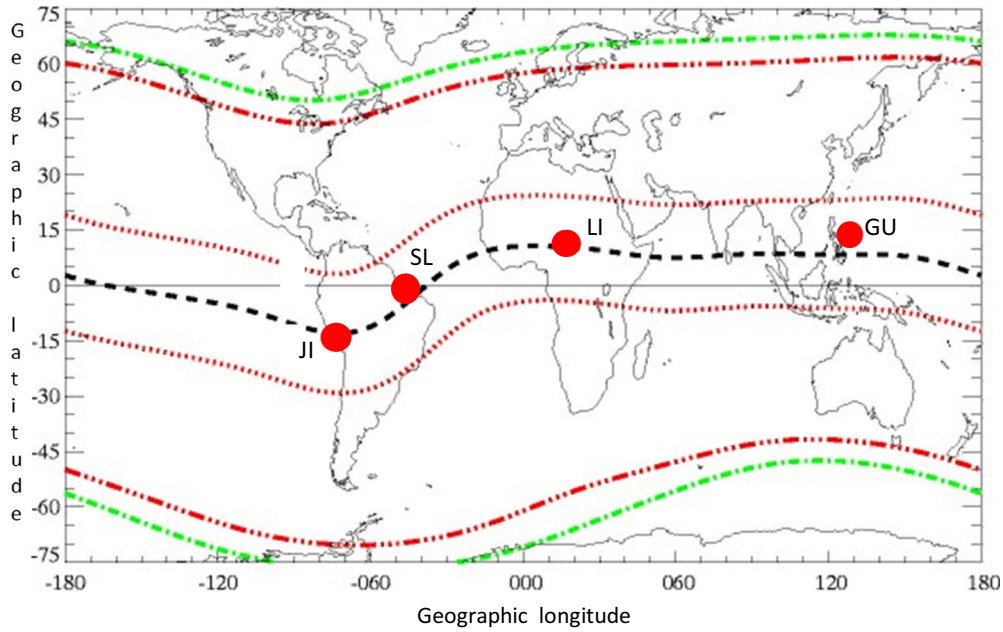

Figure 1
Map showing the locations in geographic coordinates of the stations used in the analysis

ionosphere, Fig. 3 shows the ionospheric response to the storm in terms of foF2 in black color over the stations Jicamarca, Saoluis and Guam during 25–27 August 2018. The reference day selected was 6 August (Q1, the quietest day of the month as indicated at https://wdc.kugi.kyoto-u.ac.jp/qddays). On 25 August, over Jicamarca, a small increase (maximum change $\sim$ 18%) is observed from about 16 UT (11 LT) to 21 UT (16 LT), while over Saoluis, a pronounced positive effect (maximum change $\sim$ 40%) occurs between 12 UT (09 LT) and 18 UT (15 LT), and over Guam, a short-duration positive storm effect (maximum change $\sim$ 80%) is presented between about 13 UT and 17 UT. During the main phase development, increases in foF2 are observed over Saoluis during local nighttime hours (from about 00 UT to 03 UT) and over Guam from 00 UT (10 LT) to 12 UT (22 LT) on 26 August. During the first part of the recovery, a significant positive effect starts over Jicamarca at about 12 UT (07 LT), which remains throughout the following day. Over Saoluis, two significant positive storm effects occur between 12 UT (09 LT) and 21 UT (18 LT) on August 26, and between 09 UT (06 LT) and 21 UT (18 LT) on 27 August. Over Guam, a small increase in foF2 can be observed in the daytime hours (between about 21 UT on 26 August and 09 UT on 27 August).

Figure 4 shows the corresponding hmF2 for the mentioned period. Initially, increases are observed over Jicamarca and decreases over Saoluis in association with the positive storm effects. Conversely, at Guam, no significant change in the peak height compared with the quiet conditions is observed. During the storm main phase, increases are observed over the South American stations in association with the positive effects, while hmF2 over Guam remains almost unchanged from the reference values. During the recovery, significant increases of hmF2 are clearly observed over Jicamarca alone, while over Saoluis and Guam the variations are almost the same as during the reference day.

Figure 5 presents the variations in TEC at Jicamarca, Saoluis, Guam and Libreville during the storm period 25–27 August 2018 (black color) and the corresponding values for the quiet day considered (gray color). In general, during whole storm period, decreases in TEC are observed over Jicamarca, while over Saoluis, TEC values are similar to the reference

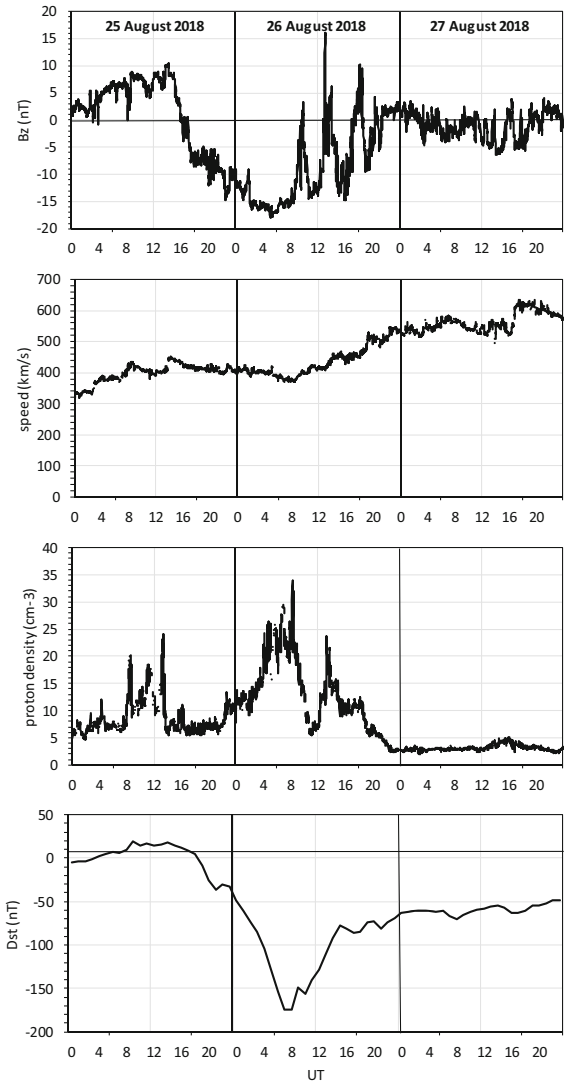

Figure 2
Variations of solar wind parameters and disturbance storm-time (Dst) index during 25–27 August 2018: (from top to bottom) the Bz component of the IMF (in nanotesla), the solar wind speed (in km/s), the proton density (in cm^{-3}) and the Dst index (in nanotesla)

ones. Over Guam, station increases are observed during the main (00–06 UT on 26 August) and recovery phases, while for Libreville, TEC increases occur during the entire storm period.

5. *Discussion*

The complete understanding of the ionospheric effects caused by geomagnetic storms is still lacking.

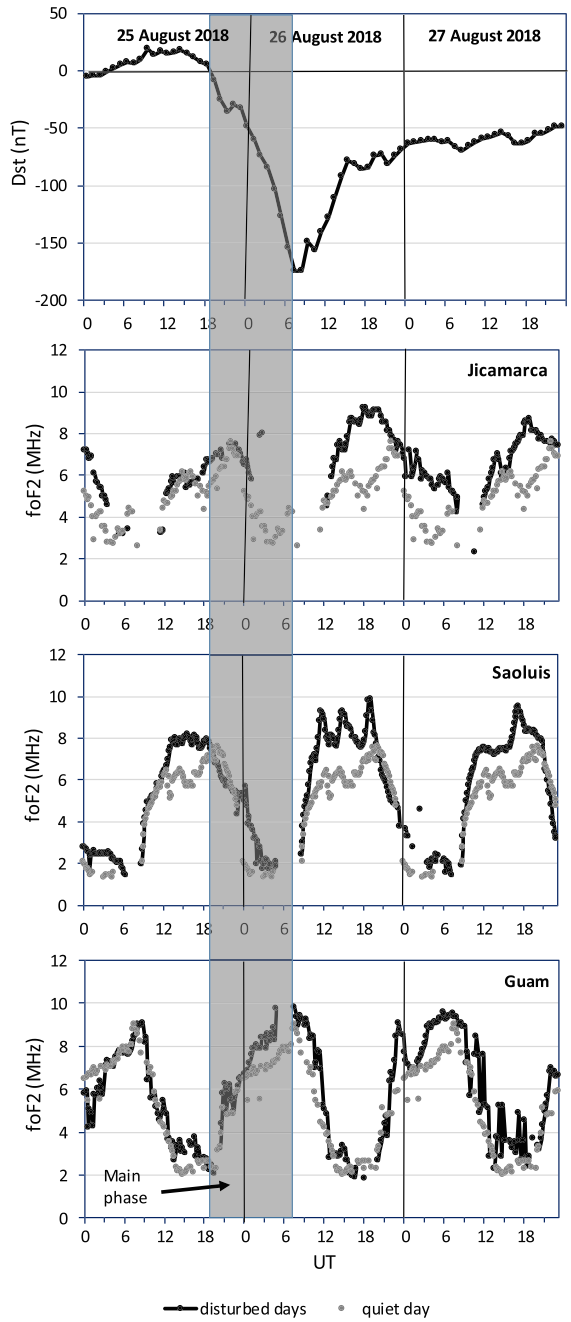

Figure 3
Variation of foF2 (in MHz) from 25 to 27 August 2018 at Jicamarca, Sao Luis and Guam. Black points correspond to storm-time values and gray points correspond to reference values. The gray rectangle indicates the storm main phase

Geomagnetic storms constitute an important link in the complex chain of solar-terrestrial relations. Although there are several common elements of

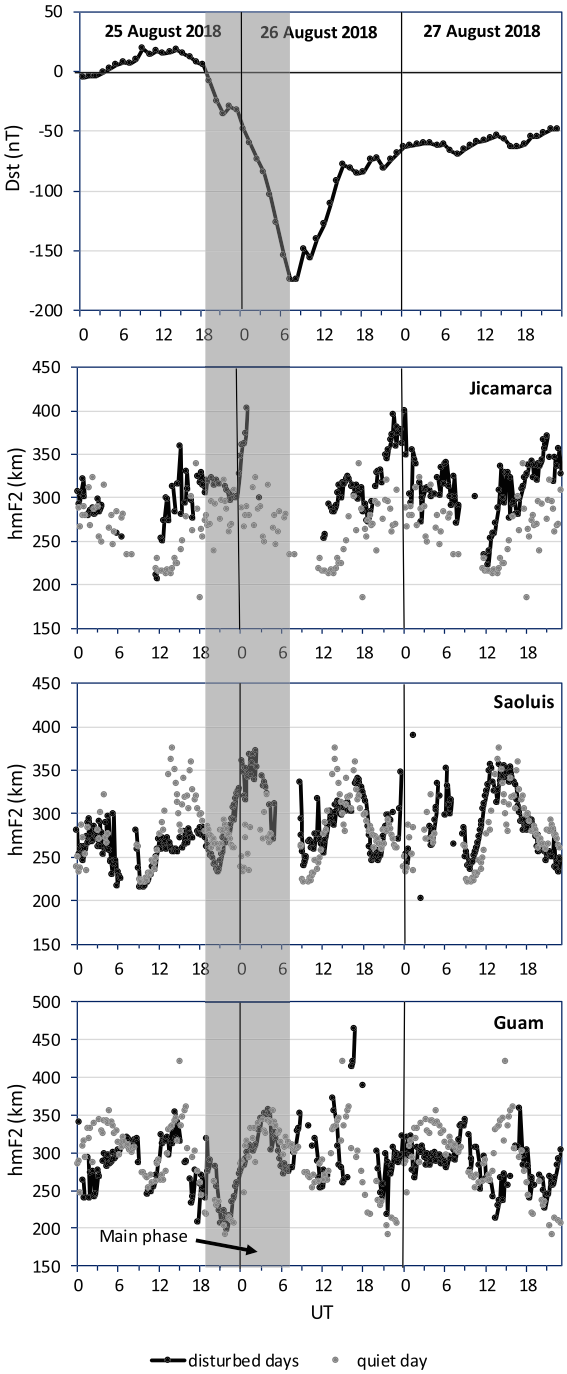

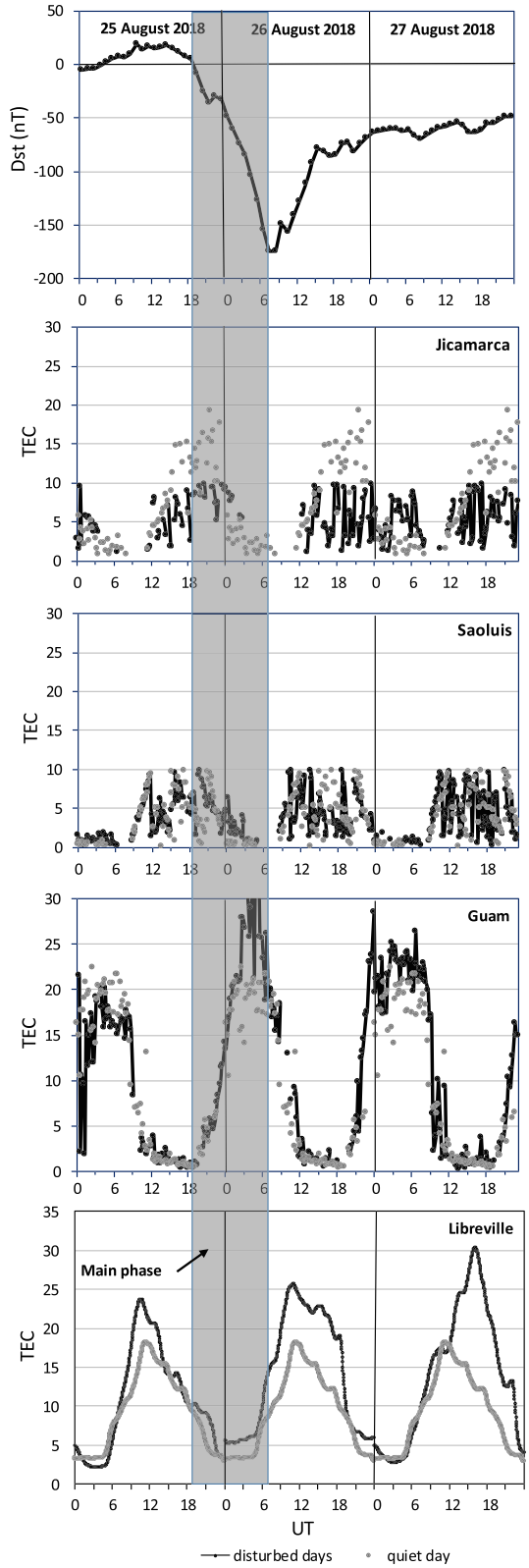

Figure 4
Variation of hmF2 (in km) from 25 to 27 August 2018 at Jicamarca, Sao Luis and Guam. Black points correspond to storm-time values, and gray points correspond to reference values. The gray rectangle indicates the storm main phase

behavior for most storms, it has been recognized that in the low-latitude and near-equator regions, the

◀Figure 5
Variation of TEC from 25 to 27 August 2018 at Jicamarca, Sao Luis, Guam and Libreville. Black points correspond to storm-time values, and gray points correspond to reference values. The gray rectangle indicates the storm main phase

ionospheric response to particular geomagnetic storms manifests some irregularities (e.g., Abdu 1997; Balan et al. 2011; Vijaya Lekshmi et al. 2011; Amaechi et al. 2018).

Our results show that the impact of the geomagnetic storm on the low-latitude ionosphere depends upon the longitude under consideration.

It is well known that prompt penetration electric fields (PPEFs) appear almost immediately in the Earth's ionosphere and magnetosphere and propagate from high to low and even equatorial latitudes. For that reason, they can play an important role over equatorial and near-equatorial latitudes during the first stage of the storm (Huang et al. 2005a, b; Tsurutani et al. 2008). These electric fields have typical lifetimes of about an hour and are highly correlated with the interplanetary magnetic field (IMF) Bz component (e.g., Gonzales et al. 1979; Fejer and Scherliess 1997; Zhao et al. 2005). When the IMF Bz is southward, it results in an eastward electric field disturbance during the day and westward during night (Kuai et al. 2015).

In order to see whether these electric fields had any effect on the initial behavior of the ionosphere, we consider first the vertical plasma drifts at 150–155-km height, recorded over Jicamarca (Peru) with the JULIA instrument. Values for 09 August (Q2 day) were considered as the quiet-time conditions because there are no drift measurements on August 6, the day taken as a reference for the other ionospheric parameters. Although these plasma drifts are measured below the F2 region, they provide meaningful information to perceive physical mechanisms of the observed ionospheric features.

Figure 6 shows the vertical plasma drifts at 150–155-km height on 25, 26 and 27 August 2018, and also on 09 August. On 25 August, the vertical drift values are different from those on 09 August at almost all times, and particularly just after 17 UT. The initial positive storm effect observed over Jicamarca from about 18 UT (13 LT) to 21 UT (16 LT) was likely initiated by a short-lived eastward prompt penetration electric field because at 17–18 UT, the upward drift velocity is significantly higher than that corresponding to 09 August. Moreover, the hmF2 values are above the reference ones during these hours. That indicates a rise of the equatorial and also low-latitude ionospheric plasma to higher altitudes where the recombination rate is slow, resulting in increased ionospheric F region electron density. However, it is not possible that the positive storm effect over Saoluis, a station close to Jicamarca, was initiated by a PPEF because their foF2 values increased prior to the storm onset (since about 12 UT) and hmF2 values are lower than the reference. At Guam, separated by about 13–15 h in local time from the South American stations, because the initial positive storm effect also started before the southward-turning IMF Bz, neither would it be initiated by a prompt penetration electric field. The uplift of ionospheric plasma over Jicamarca possibly enhances the "fountain" effect, which causes the equatorial anomaly. However, no simultaneous enhancement of the daytime total electron content is observed, as frequently occurred (e.g., Tsurutani et al. 2004; Mannucci et al. 2005; Crowley et al. 2003). On 26 August, vertical drift is downward between 17 and 19 UT (around local noon). At these hours, significant positive effects occur over Jicamarca and also over Saoluis (maximum change $\sim$ 60%). Over Jicamarca, hmF2 is increased, while over Saoluis there is practically no change compared with the reference day. On 27 August, vertical drifts exhibit an oscillating behavior: drop of $\sim$ 25 m/s at about 14:30 UT (09:30 LT) to $\sim$ 0 m/s at about 16 UT (11 LT); then it starts to increase again. Around 18 UT (14 LT), other decay is produced, reaching values near zero at 19 UT. The increase that started at 16 UT coincides with the drastic southward turning of IMF Bz, and also coincides with the beginning of another positive effect over Jicamarca.

We also have considered the eastward prompt penetration electric field model by CIRES. This model was run for the longitudes of Jicamarca and Guam. Figure 7 shows that PPEF is increased eastward over Jicamarca and increased westward over Guam at around 15 UT on 25 August. At Jicamarca,

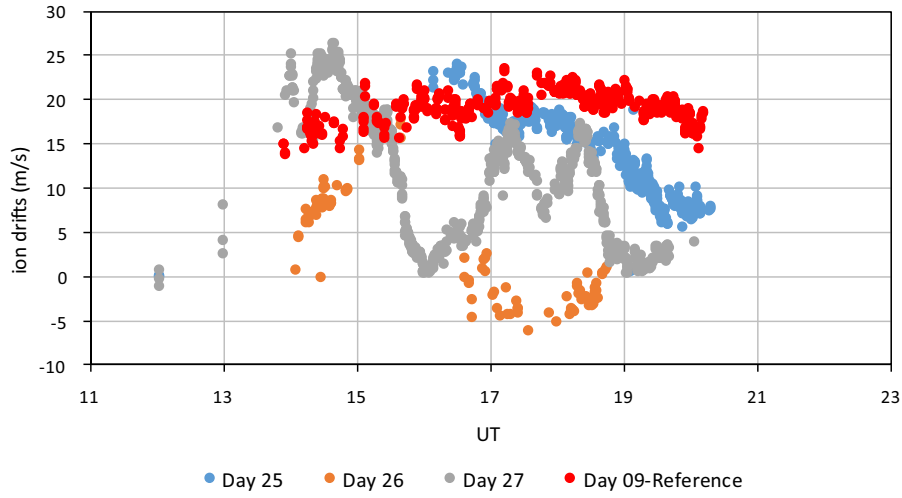

Figure 6
Vertical drifts at 150–155-km height measured over Jicamarca with the JULIA instrument on 25, 26 and 27 August 2018

there is a clear association among the increases in foF2 and the eastward peak in the PPEF (during local morning). Over Saoluis and Guam, because the enhancements in foF2 were initiated before the PPEF, this electric field possibly sometimes reinforces the initial driver of the ionospheric effects.

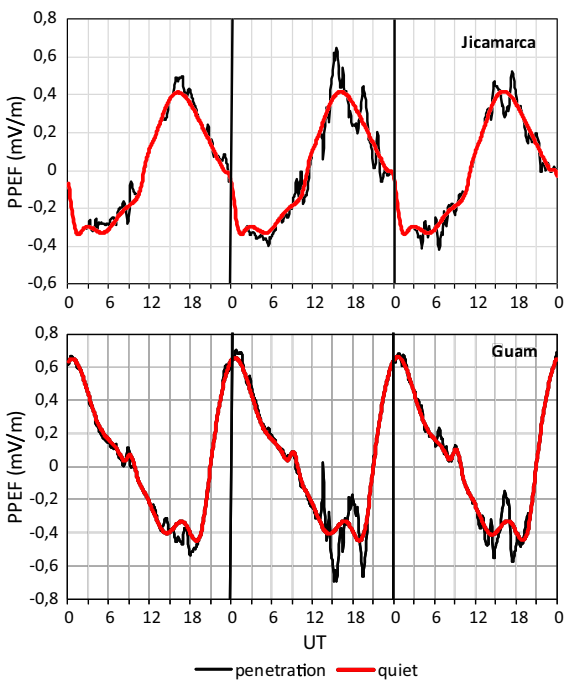

Figure 7
Prompt penetration electric field (in mV/m) at the stations Jicamarca and Guam on 25–27 August 2018. The black line corresponds to the storm time, and the gray line corresponds to a quiet magnetic day

The energy input to the auroral upper atmosphere during geomagnetic disturbances cause modifications in the neutral atmosphere circulation, which drives it equatorward. The storm-induced disturbance winds give rise to a disturbance dynamo electric field (DDEF) at middle and equatorial latitudes which is directed mainly westward on the dayside, thus reducing the ambient electric field, and eastward in post-midnight to pre-sunrise hours (Blanc and Richmond 1980; Huang et al. 2005a, b; Yamazaki and Kosch 2015). DDEFs occur about one day after major enhancement in geomagnetic activity (Scherliess and Fejer 1997). The DDEFs typically depress the ionosphere on the dayside and also suppresses the equatorial anomaly development (e.g., Abdu 1997; Richmond et al. 2003; Tsurutani et al. 2004; Maruyama et al. 2005; Xiong et al. 2016). On 26 August, during the recovery phase, over Jicamarca, a significant positive storm effect and a simultaneously increase in hmF2 during daytime hours are observed. The positive effect over Jicamarca, which is the station closest to the magnetic equator, is possibly due to a PPEF because these electric fields can continue to be in existence as long as the IMF Bz remains negative, as occurred mostly that day (Huang 2008).

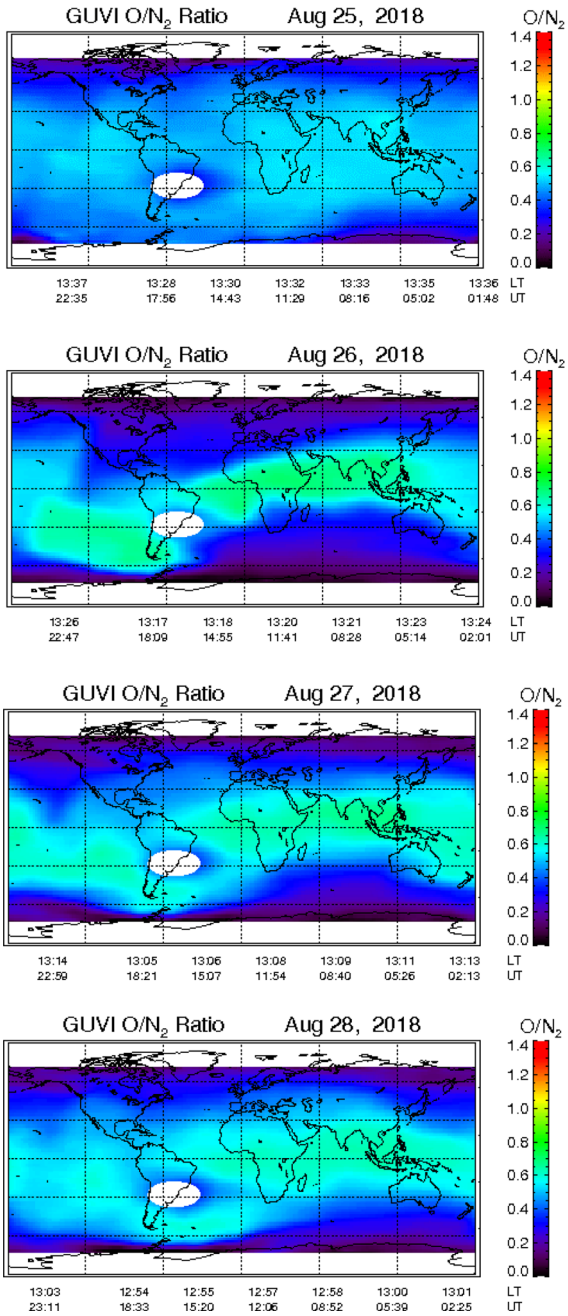

Figure 8
Global map of the O/N_2 ratio obtained by GUVI on 25–28 August 2018

Positive storm effects are also observed over Saoluis. Instead, over Guam, an eastward DDEF should produce an increase of hmF2 and also possible enhancement of electron density; however, none of these changes are observed. Scherliess and Fejer (1997) observed upward drift velocities at night with largest values near midnight and downward drifts in the sunrise-noon sector driven by dynamo processes. It is likely in this geomagnetic storm that the magnitudes of the dynamo electric fields are smaller than or comparable to the quiet-time daily variations. For that reason, any identification of the disturbance dynamo electric fields from the observations becomes difficult or impossible.

As considered below, the positive storm effects are probably due to changes in neutral gas composition. The storm-induced circulations transport air rich in atomic oxygen from higher latitudes toward lower latitudes. The enhanced oxygen density affects the ionization production, thus producing the positive storm effects.

It is important to highlight that TEC variations at Jicamarca and Saoluis do not correlate well with the F2 layer peak electron density (proportional to foF2), either during the main phase or the recovery, as is commonly accepted. For example, Liu et al. (2016) observed this for the St. Patrick's Day storm. Thus, TEC cannot always be used for the study of F2 layer dynamics during geomagnetic storms, as has been suggested (e.g., Mendillo 2006; Prölss 2006).

We should not rule out the presence of travelling atmospheric disturbances (TADs) during the main phase of the storm, which drive enhancements in foF2 in the near-equatorial latitudes, as occurred at Guam. This suggests that the storm-time response in the low-latitude ionosphere could be quite different at longitudinal sectors and thus produces different longitudinal structures, a situation that is sometimes encountered even in quiet geomagnetic conditions.

Positive ionospheric storms at low and equatorial latitudes during the recovery have also been attributed to changes in the neutral gas composition. The storm-induced, large-scale thermospheric circulation transports air rich in atomic oxygen toward lower latitudes. This enhanced oxygen density affects both the ionization production and diffusion, leading to positive storm effects (e.g., Danilov et al. 1987; Rishbeth et al. 1987; Fuller-Rowell et al. 1994; Prölss 1995). Moreover, moderate decreases of the N_2 density are also sometimes observed (e.g., Richmond and Lu 2000; Mansilla 2006). These decreases of N_2

reduce the ionospheric loss rate, which contributes to the increases of electron density. Thus, increases in the O/N_2 density ratio possibly increase the electron density, as has been suggested (e.g., Immel et al. 2001; Galav et al. 2011).

Figure 8 presents the variations in the O/N_2 ratio from GUVI measurement during 25–27 August 2018. Compared with 25 August, there is a large composition disturbance zone with a pronounced increase in the O/N_2 ratio during 26 August over the stations considered. These observations are in good agreement with what is observed in Fig. 3. The increase in O/N_2 ratio lasts throughout the day, which could be the reason for increased electron density over Saoluis and Guam. Over Jicamarca, the composition change possibly replaces the neutral wind and the electric field effects, which play significant roles in the ionospheric disturbance. The increase in the O/N_2 ratio is likely caused by an increase in the atomic oxygen, which is lighter than molecular nitrogen and reaches low and equatorial latitudes earlier.

These compositional changes seem to move into the dayside due to a co-rotation effect because the increase of density occurs over Saoluis on August 26 from morning until afternoon hours and at Guam during daytime on August 27.

6. Conclusions

The study of the ionospheric response at near-magnetic-equator latitudes during the geomagnetic storm of 26 August 2018 revealed some interesting features.

We have observed pre-storm enhancements, which could be due to previous moderate geomagnetic activity. Moreover, only one station (Jicamarca) clearly reveals a prompt penetration electric field effect when Bz turned strongly negative during the initial phase of the storm. Over the stations Saoluis and Guam, a PPEF effect is not evident. These stations presented pre-storm enhancements in foF2. Furthermore, in this case study, disturbed dynamo electric fields appear not to have played a crucial role in increasing electron density near equatorial regions during the recovery phase because the observed disturbances did not correspond with those produced by these electric fields, that is, negative (positive) storm effects on the dayside (night). Finally, the increases in electron density observed during recovery are likely caused by neutral composition changes.

This work also shows that the storm-time response of the equatorial ionosphere can be quite different at locations separated in longitude by as small as 2 h in local time.

However, due to the complex interplay among the different drivers, it is often difficult to distinguish one driving force from another based on observations alone. Thus, more observations are required to distinguish between the different mechanisms for pre-storm enhancements as well as the relative importance of the mechanisms involved during the different phases of the storms.

References

Abdu, M. A. (1997). Major phenomena of the equatorial ionosphere–thermosphere system under disturbed conditions. *Journal of Atmospheric and Solar Terrestrial Physics, 59,* 1505–1519.

Abdu, M. A., Maruyama, T., Batista, I. S., Saito, S., & Nakamura, M. (2007). Ionospheric responses to the October 2003 superstorm: Longitude/local time effects over equatorial low and middle latitudes. *Journal of Geophysical Research, 112,* A10306. https://doi.org/10.1029/2006JA012228

Amaechi, P. O., Oyeyemi, E. O., & Akala, A. O. (2018). The response of African equatorial/low-latitude ionosphere to 2015 St Patrick's Day geomagnetic storm. *Space Weather, 16,* 601–618.

Astafyeva, E., Zakharenkova, I., & Förster, M. (2015). Ionospheric response to the 2015 St Patrick's Day storm: A global multi-instrumental overview. *Journal of Geophysical Research: Space Physics, 120,* 9023–9037.

Balan, N., Yamamoto, M., Sreeja, V., Batista, I. S., Lynn, K. J. W., Abdu, M. A., et al. (2011). A statistical study of the response of the dayside equatorial F_2 layer to the main phase of intense geomagnetic storms as an indicator of penetration electric field. *Journal of Geophysical Research, 116,* A03323.

Blanc, M., & Richmond, A. D. (1980). The ionospheric disturbance dynamo. *Journal of Geophysical Research, 85,* 1669–1686.

Buonsanto, M. J. (1999). Ionospheric storms—a review. *Space Science Reviews, 88,* 563–601.

Crowley, G., Hackert, C. L., Meier, R. R., Strickland, D. J., Paxton, L. J., Pi, X., et al. (2006). Global thermosphere-ionosphere response to onset of 20 November 2003 magnetic storm. *Journal*

of Geophysical Research, 111, A10S18. https://doi.org/10.1029/2005JA011518

Danilov, A., Morozova, L. D., Dachev, T. C., & Kutiev, I. (1987). Positive phase of ionospheric storms and its connection with the dayside cusp. *Advances in Space Research, 7*(8), 81–88.

Fejer, B. G., & Emmert, J. T. (2003). Low-latitude ionospheric disturbance electric field effects during the recovery phase of the 19–21 October 1998 magnetic storm. *Journal of Geophysical Research, 108*(A12), 1454. https://doi.org/10.1029/2003JA010190

Fejer, B. G., Jensen, J. W., & Su, S.-Y. (2008). Seasonal and longitudinal dependence of equatorial disturbance vertical plasma drifts. *Geophysical Research Letters, 35,* L20106. https://doi.org/10.1029/2008GL035584

Fejer, B. G., Larsen, M. F., & Farley, D. T. (1983). Equatorial disturbance dynamo electric fields. *Geophysical Research Letters, 10,* 537–540.

Fejer, B. G., & Scherliess, L. (1997). Empirical models of storm time equatorial zonal electric fields. *Journal of Geophysical Research, 102,* 24047–24056.

Fuller-Rowell, T. J., Codrescu, M. V., & Moffett, R. J. (1994). Response of the thermosphere and ionosphere to geomagnetic storms. *Journal of Geophysical Research, 99,* 3893–4011.

Galav, P., Sharma, S., & Pandey, R. (2011). Study of simultaneous penetration of electric fields and variation of total electron content in the day and night sectors during the geomagnetic storm of 23 May 2002. *Journal of Geophysical Research, 116,* A12324.

Gonzales, C. A., Kelley, M. C., Fejer, B. G., Vickrey, J. F., & Woodman, R. F. (1979). Equatorial electric fields during magnetically disturbed conditions: 2. Implications of simultaneous auroral and equatorial measurements. *Journal of Geophysical Research*, *84*(A10), 5803–5812. https://doi.org/10.1029/JA084iA10p05803.

Huang, C. S. (2008). Continuous penetration of the interplanetary electric field to the equatorial ionosphere over eight hours during intense geomagnetic storms. *Journal of Geophysical Research, 113,* A11305. https://doi.org/10.1029/2008JA013588

Huang, C. M. (2013). Disturbance dynamo electric fields in response to geomagnetic storms occurring at different universal times. *Journal of Geophysical Research Space Physics, 118,* 496–501. https://doi.org/10.1029/2012JA018118

Huang, C.-S., Foster, J. C., Goncharenko, L. P., Erickson, P. J., & Rideout, W. (2005). A strong positive phase of ionospheric storms observed by the Millstone Hill incoherent scatter radar and global GPS network. *Journal of Geophysical Research, 110,* A06303.

Huang, C. M., Richmond, A. D., & Chen, M. Q. (2005). Theoretical effects of geomagnetic activity on low-latitude ionospheric electric fields. *Journal of Geophysical Research, 110,* A05312. https://doi.org/10.1029/2004JA010994

Huang, C.-S., Sazykin, S., Chau, J. L., Maruyama, N., & Kelley, M. C. (2007). Penetration electric fields: Efficiency and characteristic time scale. *Journal of Atmospheric and Terrestrial Physics, 69*(10–11), 1135–1146. https://doi.org/10.1016/j.jastp.2006.08.016

Immel, T. J., Crowley, G., Craven, J. D., & Roble, R. G. (2001). Day side enhancements of thermospheric O/N2 following magnetic storm onset. *Journal of Geophysical Research, 106,* 15471–15488.

Klimenko, M. V., Klimenko, V. V., Ratovsky, K. G., Goncharenko, L. P., Sahai, Y., Fagundes, P. R., et al. (2011). Numerical modeling of ionospheric effects in the middle- and low-latitude F region during geomagnetic storm sequence of 9–14 September 2005. *Radio Science, 46,* RS0D03. https://doi.org/10.1029/2010RS004590

Kuai, J., Liu, L., Lei, J., Liu, J., Zhao, B., Chen, Y., et al. (2017). Regional differences of the ionospheric response to the July 2012 geomagnetic storm. *Journal of Geophysical Research Space Physics, 122,* 4654–4668. https://doi.org/10.1002/2016JA023844

Kuai, J., Liu, L., Liu, J., Zhao, B., Chen, Y., Le, H., & Wan, W. (2015). The long-duration positive storm effects in the equatorial ionosphere over Jicamarca. *Journal of Geophysical Research Space Physics, 120,* 1311–1324. https://doi.org/10.1002/2014JA020552

Liu, J., Wang, W., Burns, A., Yue, X., Zhang, S., Zhang, Y., & Huang, C. (2016). Profiles of ionospheric storm-enhanced density during the 17 March 2015 great storm. *Journal of Geophysical Research Space Physics, 121,* 727–744. https://doi.org/10.1002/2015JA021832

Mansilla, G. A. (2006). Equatorial and low latitude ionosphere during intense geomagnetic storms. *Journal of Atmospheric and Solar-Terrestrial Physics, 68,* 2091–2100.

Mannucci, A. J., Tsurutani, B. T., Iijima, B. A., Komjathy, A., Saito, A., Gonzalez, W. D., et al. (2005). Dayside global ionospheric response to the major interplanetary events of October 29–30, 2003 "Halloween Storms". *Geophysical Research Letters*, *32*, L12S02. https://doi.org/10.1029/2004GL021467.

Maruyama, N., Richmond, A. D., Fuller-Rowell, T. J., Codrescu, M. V., Sazykin, S., Toffoletto, F. R., et al. (2005). Interaction between direct penetration and disturbance dynamo electric fields in the storm-time equatorial ionosphere. *Geophysical Research Letters, 32,* L17105. https://doi.org/10.1029/2005GL023763

Mayr, H. G., & Volland, H. (1972). Magnetic storm effects in the neutral composition. *Planetary and Space Science, 20,* 379–393.

Mendillo, M. (2006). Storms in the ionosphere: Patterns and processes for total electron content. *Reviews of Geophysics, 44,* RG4001.

Nishida, A. (1968). Coherence of geomagnetic DP 2 fluctuations with interplanetary magnetic variations. *Journal of Geophysical Research, 73,* 5549–5559.

Pedatella, N. M., Forbes, J. M., Lei, J., Thayer, J. P., & Larson, K. M. (2008). Changes in the longitudinal structure of the low-latitude ionosphere during the July 2004 sequence of geomagnetic storms. *Journal of Geophysical Research, 113,* A11315. https://doi.org/10.1029/2008JA013539

Prölss, G. W. (1987). Storm-induced changes in the thermospheric composition at middle latitudes. *Planetary and Space Science, 35,* 807–811.

Prölss, G. W. (1995). Ionospheric F-region storms. *Handbook of atmospheric electrodynamics, Vol 2* (pp. 195–248). Boca Raton: CRC Press.

Prölss, G. W., Magnetic storm associated perturbations of the upper atmosphere, in Magnetic Storms, Geophys. Monogr. Ser., vol. 98, edited by B. T. Tsurutani et al. pp. 227–241, AGU, Washington, D. C., 1997.

Prölss, G. W. (2006). Ionospheric F-region Storms: Unsolved problems. In *Characterising the Ionosphere* (pp. 10-1–10-20). Meeting Proceedings RTO-MP-IST-056, Paper 10. Neuilly-sur-Seine, France: RTO. Available from: http://www.rto.nato.int/abstracts.asp.

Richmond, A. D., & Lu, G. (2000). Upper-atmospheric effects of magnetic storms: A brief tutorial. *Journal of Atmospheric and Solar-Terrestrial Physics, 62,* 1115–1127.

Richmond, A. D., Peymirat, C., & Roble, R. G. (2003). Long-lasting disturbance in the equatorial ionospheric electric field simulated with a coupled magnetosphere–ionosphere–thermosphere model. *Journal of Geophysical Research, 108*(A3), 1118.

Rishbeth, H., Fuller-Rowell, T. J., & Rodger, A. S. (1987). F-layer storms and thermospheric composition. *Physica Scripta, 36,* 327–336.

Sahai, Y., Fagundes, P. R., Becker-Guedes, F., Bolzan, M. J. A., Abalde, J. R., Pillat, V. G., et al. (2005). Effects of the major geomagnetic storms of October 2003 on the equatorial and low-latitude F region in two longitudinal sectors. *Journal of Geophysical Research, 110,* A12S91. https://doi.org/10.1029/2004JA010999

Santos, A. M., Abdu, M. A., Sobral, J. H. A., Koga, D., Nogueira, P. A. B., & Candido, C. M. N. (2012). Strong longitudinal difference in ionospheric responses over Fortaleza (Brazil) and Jicamarca (Peru) during the January 2005 magnetic storm, dominated by northward IMF. *Journal of Geophysical Research, 117,* A08333. https://doi.org/10.1029/2012JA017604

Sastri, J. H., Abdu, M. A., & Sobral, J. H. A. (1997). Response of equatorial ionosphere to episodes of asymmetric ring current activity. *Annales Geophysicae, 15,* 1316–1323.

Scherliess, L., & Fejer, B. G. (1997). Storm time dependence of equatorial disturbance dynamo zonal electric fields. *Journal of Geophysical Research, 102*(A12), 24037–24046.

Sezen, U., Arikan, F., Arikan, O., Ugurlu, O., & Sadeghimorad, A. (2013). Online, automatic, near-real time estimation of GPS-TEC: IONOLAB-TEC. *Space Weather, 11,* 297–305. https://doi.org/10.1002/swe.20054

Tsurutani, B., Mannucci, A., Iijima, B., Abdu, M. A., Sobral, J. H. A., Gonzalez, W., et al. (2004). Global dayside ionospheric uplift and enhancement associated with interplanetary electric fields. *Journal of Geophysical Research, 109,* A08302.

Tsurutani, B. T., Verkhoglyadova, O. P., Mannucci, A. J., Saito, A., Araki, T., Yumoto, K., et al. (2008). Prompt penetration electric fields (PPEFs) and their ionospheric effects during the great magnetic storm of 30–31 October 2003. *Journal of Geophysical Research, 113,* A05311.

Vijaya Lekshmi, D., Balan, N., Tulasi Ram, S., & Liu, J. Y. (2011). Statistics of geomagnetic storms and ionospheric storms at low and mid latitudes in two solar cycles. *Journal of Geophysical Research, 116,* A11328.

Xiong, C., Luhr, H., & Fejer, B. G. (2016). The response of equatorial electrojet, vertical plasma drift, and thermospheric zonal wind to enhanced solar wind input. *Journal of Geophysical Research Space Physics, 121,* 5653–5663. https://doi.org/10.1002/2015JA022133

Yamazaki, Y., & Kosch, M. J. (2015). The equatorial electrijet during geomagnetic storms and substorms. *Journal of Geophysical Research Space Physics, 120,* 2276–2287. https://doi.org/10.1002/2014JA020773

Zhao, B., Wan, W., & Liu, L. (2005). Responses of equatorial anomaly to the October−November 2003 superstorms. *Annales Geophysicae, 23,* 693–706.

Zhou, Y.-L., Lühr, H., Xiong, C., & Pfaff, R. F. (2016). Ionospheric storm effects and equatorial plasma irregularities during the 17–18 March 2015 event. *Journal of Geophysical Research Space Physics, 121,* 9146–9163. https://doi.org/10.1002/2016JA023122

Zolotukhina, N., Polekh, N., Kurkin, V., Rogov, D., Romanova, E., & Chelpanov, M. (2017). Ionospheric effects of St. Patrick's storm over Asian Russia: 17–19 March 2015. *Journal of Geophysical Research: Space Physics, 122,* 2484–2504. https://doi.org/10.1002/2016JA023180

(Received April 3, 2020, revised September 23, 2020, accepted October 8, 2020, Published online October 19, 2020)